JOURNAL OF Materials CHEMISTRY

Hybrid open frameworks (MIL-*n*). Part 4† Synthesis and crystal structure of MIL-8, a series of lanthanide glutarates with an open framework, $[Ln(H_2O)]_2[O_2C(CH_2)_3CO_2]_3 \cdot 4H_2O$

F. Serpaggi and G. Férey*

Institut Lavoisier, UMR CNRS 173, Université de Versailles Saint-Quentin-en-Yvelines, 45, avenue des Etats-Unis, 78035 Versailles Cedex, France. E-mail: ferey@chimie.uvsq.fr

Received 9th April 1998, Accepted 17th September 1998

The first series of rare-earth carboxylates with an open framework has been prepared hydrothermally (180 °C, 3 days) by the action of glutaric acid on the metal chlorides in the presence of base. The crystal structure of the neodymium compound $[Nd^{III}(H_2O)]_2[O_2C(CH_2)_3CO_2]_3 \cdot 4H_2O$ has been determined by single-crystal X-ray diffraction. The composite material crystallizes in the monoclinic space group $C2/c$ (no. 15) with $a=8.1174(1)$ Å, $b=15.1841(3)$ Å, $c=19.8803(3)$ Å, $\beta=93.762(1)°$ (final agreement factors $R_1=0.0279$, $wR_2=0.0693$). The organic–inorganic network is three-dimensional and consists of chains of edge-sharing rare-earth polyedra $NdO_8(H_2O)$ along the [100] direction, linked together by the carbon chains along two directions. The connection involves the formation of channels parallel to the rare-earth chains in which weakly bonded water molecules are incorporated. The analogous compounds were obtained with Pr, Sm, Eu, Gd, Dy, Ho and Y.

Introduction

Since 1992, the ULM-*n* ($n \leqslant 19$) series of fluorinated microporous gallophosphates that our group discovered and characterized structurally led us to propose a hypothesis for the mechanism of their formation[1] from solution during their templated synthesis. Indeed, the structural studies showed that the inorganic skeleton of the porous solids was built up from a small number of well defined oligomers with a formal charge of -2 (mainly gallophosphate tetramers Ga_2P_2 and hexamers Ga_3P_3). The hypothesis therefore claimed that the same oligomers existed in the solution and that the charge density of the protonated amine was the driving force of the synthesis. In the solution, we assumed that it controlled (i) the extent of the oligomeric condensation of monophosphate complexes of the gallium species up to the equalization of the charge densities of the amine and the oligomer and (ii) the formation of a neutral ion pair which allows the infinite condensation and therefore the formation of the solid. The structure of the latter, which depends on the volume and the plasticity of the pair, is obtained using criteria of minimization of the lattice energy. This hypothesis has just received a few weeks ago its first experimental proof by Taulelle and coworkers[2] by *in situ* NMR experiments under hydrothermal conditions.

Before this result, and considering that this hypothesis was true, we found for the first time some hitherto unknown magnetic microporous iron and vanadium phosphates,[3] in which the total substitution of Ga by Fe or V induces new structural types. Supplementary work is currently in progress in this field with the use of other 3d transition metals. The extension of this idea to microporous rare earth phosphates unfortunately failed owing to the strong affinity of phosphate and fluoride anions towards lanthanide elements which, whatever the chemical conditions, leads to the formation of monazite type phosphates $LnPO_4$ and fluorides LnF_3.

In order to obtain lanthanide compounds with an open framework, it was then necessary to change our strategy and substitute phosphate anions by other chelating agents which prevent the formation of dense, insoluble inorganic species. This is the case for phosphonates and since the work of Alberti, Dines and Clearfield, it is well known that these species react with inorganic compounds.[4] While most of the papers cited in the literature concern non-functionalized monophosphonates, with the aim of synthesizing layered compounds,[5] some attempts with diphosphonates[6] and monophosphonates functionalized with $-CO_2H$ or $-NH_2$ groups[7] led to a few three-dimensional compounds. The chelating power of the diphosphonate group generally leads to a pillaring between inorganic layers or chains. This property can be utilised as a general method for obtaining composite solids in which the skeleton is built up simultaneously by organic and inorganic species. This approach can present three advantages: (i) owing to the large number of commercial phosphonates and the possibility to prepare some of them by the Arbuzov reaction, a large modulation of the open framework character of the corresponding materials may be expected, (ii) it can allow non-templated syntheses of microporous samples, and (iii) this strategy can be extended to other chelating agents different from phosphonates such as sulfonates and carboxylates. Complexation of the lanthanide elements by carboxylates has already been studied and usually leads to the formation of clusters, some of which have been structurally characterized.[8] To our knowledge, only two-dimensional rare-earth oxalates have been mentioned previously,[9] and no three-dimensional lanthanide carboxylates with longer carbon chains have been reported. We report here the hydrothermal preparation and the crystal structure determination of the first three-dimensional lanthanide glutarates.

Experimental

Reagents

$LnCl_3 \cdot xH_2O$ ($x=6$ or 7) (Aldrich, 99.9%), glutaric acid ($HO_2C(CH_2)_3CO_2H$, Aldrich, 99%), and 1,3-diaminopropane [$H_2N(CH_2)_3NH_2$, Aldrich, 99%] were used as received with no further purification.

Preparation of lanthanide glutarates

Neodymium glutarate, $[Nd(H_2O)]_2[O_2C(CH_2)_3CO_2]_3 \cdot 4H_2O$, was hydrothermally synthesized in a 23 ml Teflon-lined Parr bomb under autogeneous pressure (180 °C, 3 days). The starting reagents were neodymium(III) chloride hexahydrate ($NdCl_3 \cdot 6H_2O$, Aldrich, 99.9%), glutaric acid [HO_2C-

---

†Part 3: preceding paper.

$(CH_2)_3CO_2H$, Aldrich, 99%; $pK_a(1)=4.31$ and $pK_a(2)=5.41$[10]], 1,3-diaminopropane $[H_2N(CH_2)_3NH_2$, Aldrich, 99%] and distilled water. The molar ratio was 1 $NdCl_3·6H_2O$: 1 $HO_2C(CH_2)_3CO_2H$: 1.3 $H_2N(CH_2)_3NH_2$: 100 H_2O. Neodymium chloride and glutaric acid were first dissolved separately in 2 ml H_2O. The amine was added to the glutaric acid solution which was then mixed with the neodymium chloride solution. The initial pH was 6 (this pH value was reached by the addition of the amine and was selected in order to deprotonate both acid groups of the diacid) and the resulting pH was 5–6. The replacement of 1,3-diaminopropane by different bases (NaOH, NH_3, ethylenediamine, tetramethylammonium hydroxide) led to the same product. The crystalline product obtained was filtered off, washed with distilled water and dried at room temperature. Similar procedures were used to obtain the analogous compounds with Pr, Sm, Eu, Gd, Dy, Ho and Y.

X-Ray data collection

X-Ray powder diffraction (XRD) data were collected on a Siemens D5000 diffractometer with Cu-Kα radiation, in the range $5<2\theta<60°$, with step size 0.04° (2θ) and acquisition with steps of 1 s (Fig. 1).

Thermogravimetry

TG analysis was carried out on a TA Instrument type 2050 thermoanalyzer under O_2 gas flow with a heating rate of 5 °C min^{-1}, from 30 to 900 °C.

IR spectroscopy

FTIR spectra were obtained on a Nicolet Magna-IR™ 550 spectrometer with the usual KBr pellet technique.

Structure determination

A suitable single-crystal for X-ray analysis was mounted with Araldite on a glass fiber. The intensity data were collected on a Siemens SMART three-circle diffractometer equipped with a CCD bidimensional detector. The crystal-to-detector distance was 45 mm allowing for data collection up to 65° (2θ). Slightly more than one hemisphere of data were recorded. Crystal data and details of the data collection for $[Nd(H_2O)]_2[O_2C(CH_2)_3CO_2]_3·4H_2O$ are given in Table 1. An empirical absorption correction was applied using the SADABS program[11] based on the method of Blessing.[12] The cell was found to be monoclinic, space group $C2/c$ (no. 15), $a=8.1174(1)$ Å, $b=15.1841(3)$ Å, $c=19.8803(3)$ Å, $\beta=93.762(1)°$. The structure was solved using direct methods of the SHELXTL package.[13] Nd and O atoms were first located and C atoms were found from difference-Fourier maps. Hydrogen atoms were refined with geometrical constraints.

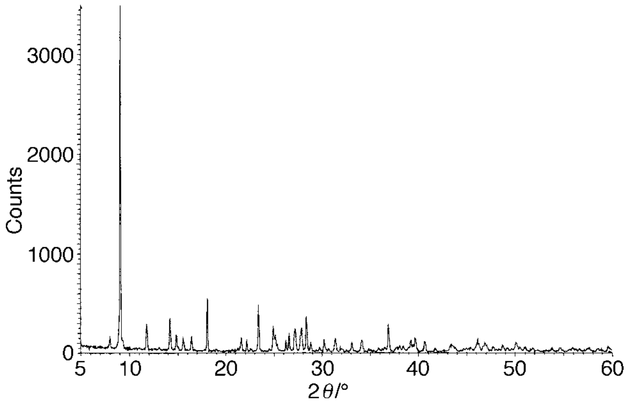

Fig. 1 X-Ray pattern for $[Nd(H_2O)]_2[O_2C(CH_2)_3CO_2]_3·4H_2O$.

Table 1 Crystal data and structure refinement for $[Nd(H_2O)]_2[O_2C(CH_2)_3CO_2]_3·4H_2O$

Empirical formula	$C_{15}H_{30}Nd_2O_{18}$
Formula weight	786.86
Temperature/K	293(2)
Wavelength/Å	0.71073
Crystal system	Monoclinic
Space group	$C2/c$ (no. 15)
Unit cell dimensions	
a/Å	8.1174(1)
b/Å	15.1841(3)
c/Å	19.8803(3)
β/degrees	93.762(1)
Volume/Å^3, Z	2445.07(7), 4
D_c/g cm^{-3}	2.138
Absorption coefficient/mm^{-1}	4.282
$F(000)$	1536
Crystal size/mm	0.3 × 0.2 × 0.16
θ range for data collection/degrees	3.38–32.24
Limiting indices	$-11\leqslant h\leqslant 11$, $-15\leqslant k\leqslant 22$, $-29\leqslant l\leqslant 21$
Reflections collected	9823
Independent reflections	4095 ($R_{int}=0.0294$)
Refinement method	Full-matrix least-squares on F^2
Data/restraints/parameters	4095/0/160
Goodness-of-fit on F^2	1.152
Final R indices [$I>2\sigma(I)$]	$R_1=0.0279$, $wR_2=0.0681$
R indices (all data)	$R_1=0.0307$, $wR_2=0.0693$
Extinction coefficient	0.0011(1)
Largest diff. peak and hole/e Å^{-3}	1.435 and −1.251

The final reliability factors converged to $R_1=0.0279$ and $wR_2=0.0693$. Final positional parameters and intramolecular distances and angles are given in Tables 2 and 3. The cell parameters for the isotypic Pr, Nd, Sm, Eu, Gd, Dy, Ho and Y compounds are summarized in Table 4.

Full crystallographic details, excluding structure factors, have been deposited at the Cambridge Crystallographic Data

Table 2 Atomic coordinates and equivalent isotropic displacement parameters (Å^2) for $[Nd(H_2O)]_2[O_2C(CH_2)_3CO_2]_3·4H_2O$

Atom	x	y	z	U_{eq}[a]
Nd	0.2456(1)	0.0377(1)	0.4881(1)	0.016(1)
O1	0.5142(3)	0.0448(1)	0.4384(1)	0.024(1)
O2	0.2319(3)	−0.0496(2)	0.5943(1)	0.034(1)
O3	−0.0150(2)	0.0797(1)	0.5344(1)	0.024(1)
O4	0.2661(2)	−0.1158(1)	0.4401(1)	0.029(1)
O5	0.1534(3)	0.0551(2)	0.3665(1)	0.029(1)
O6	0.1679(3)	0.1778(1)	0.4258(1)	0.026(1)
Ow1	0.3882(3)	0.1483(2)	0.5619(1)	0.032(1)
Ow2	0.607(1)	−0.4081(4)	0.6992(3)	0.181(4)
Ow3	0.875(1)	−0.4304(7)	0.7825(6)	0.223(5)
C1	0.3798(3)	−0.0742(2)	0.6015(1)	0.018(1)
C2	0.4283(4)	−0.1410(2)	0.6554(2)	0.022(1)
C3	0.3594(5)	−0.2332(2)	0.6356(2)	0.029(1)
C4	−0.0518(4)	0.2256(2)	0.5782(2)	0.030(1)
C5	−0.1157(3)	0.1359(2)	0.5568(2)	0.020(1)
C6	0.1334(3)	0.1379(2)	0.3701(2)	0.020(1)
C7	0.0746(4)	0.1903(2)	0.3080(2)	0.024(1)
C8	0	0.1340(3)	¼	0.027(1)
H2A	0.3856(4)	−0.1228(2)	0.6977(2)	0.026
H2B	0.5476(4)	−0.1438(2)	0.6618(2)	0.026
H3A	0.3705(5)	−0.2716(2)	0.6746(2)	0.035
H3B	0.2427(5)	−0.2281(2)	0.6221(2)	0.035
H4A	−0.0620(4)	0.2647(2)	0.5396(2)	0.036
H4B	0.0647(4)	0.2206(2)	0.5920(2)	0.036
H7A	0.1672(4)	0.2231(2)	0.2923(2)	0.029
H7B	−0.0074(4)	0.2326(2)	0.3206(2)	0.029
H8A	0.0851(4)	0.0964(3)	0.2335(2)	0.033
H8B	−0.0851(4)	0.0964(3)	0.2665(2)	0.033

[a] U_{eq} is defined as one third of the trace of the orthogonalized U_{ij} tensor.)

Table 3 Bond lengths (Å) and angles (degrees) for $[Nd(H_2O)]_2[O_2C(CH_2)_3CO_2]_3 \cdot 4H_2O$[a]

Nd–O3	2.445(2)	C1–C2	1.508(4)
Nd–O1	2.455(2)	C2–C3	1.549(4)
Nd–Ow1	2.467(2)	C3–C4^{c}	1.524(4)
Nd–O5	2.498(2)	C4^{c}–C5^{c}	1.509(4)
Nd–O2	2.500(2)	C5^{c}–O3^{c}	1.282(3)
Nd–O6	2.521(2)	C5^{c}–O4^{d}	1.264(3)
Nd–O4	2.529(2)	C6–O5	1.270(3)
Nd–O3^{a}	2.602(2)	C6–O6	1.278(3)
Nd–O1^{b}	2.671(2)	C6–C7	1.518(4)
C1–O1^{b}	1.288(3)	C7–C8	1.528(4)
C1–O2	1.257(3)		
O3–Nd–O1	162.32(7)	Ow1–Nd–O1^{b}	72.37(7)
O3–Nd–Ow1	89.02(8)	O5–Nd–O1^{b}	137.79(7)
O1–Nd–Ow1	79.32(8)	O2–Nd–O1^{b}	50.29(7)
O3–Nd–O5	97.17(8)	O6–Nd–O1^{b}	144.57(7)
O1–Nd–O5	79.78(8)	O4–Nd–O1^{b}	73.15(7)
Ow1–Nd–O5	126.99(8)	O3^{a}–Nd–O1^{b}	105.31(7)
O3–Nd–O2	74.55(8)	C1^{b}–O1–Nd	155.6(2)
O1–Nd–O2	116.96(7)	C1^{b}–O1–Nd^{b}	90.3(2)
Ow1–Nd–O2	84.53(9)	Nd–O1–Nd^{b}	113.25(8)
O5–Nd–O2	147.80(9)	C1–O2–Nd	99.2(2)
O3–Nd–O6	76.70(7)	C5–O3–Nd	153.1(2)
O1–Nd–O6	87.98(7)	C5^{a}–O3^{a}–Nd	92.7(2)
Ow1–Nd–O6	79.04(8)	Nd–O3–Nd^{a}	112.75(8)
O5–Nd–O6	52.07(7)	C5^{a}–O4–Nd	96.6(2)
O2–Nd–O6	146.97(8)	C6–O5–Nd	94.7(2)
O3–Nd–O4	117.55(7)	C6–O6–Nd	93.5(2)
O1–Nd–O4	78.83(7)	O2–C1–O1^{b}	119.9(3)
Ow1–Nd–O4	144.28(7)	O2–C1–C2	118.9(2)
O5–Nd–O4	75.83(8)	O1^{b}–C1–C2	121.1(2)
O2–Nd–O4	80.66(9)	C1–C2–C3	110.7(3)
O6–Nd–O4	127.80(8)	C2–C3–C4^{c}	112.4(3)
O3–Nd–O3^{a}	67.25(8)	C3–C4^{c}–C5^{c}	114.3(3)
O1–Nd–O3^{a}	127.50(7)	O4^{d}–C5^{c}–O3^{c}	119.8(3)
Ow1–Nd–O3^{a}	150.79(8)	O4^{d}–C5^{c}–C4^{c}	121.3(2)
O5–Nd–O3^{a}	74.92(8)	O3^{c}–C5^{c}–C4^{c}	118.9(2)
O2–Nd–O3^{a}	73.20(8)	O5–C6–O6	119.7(3)
O6–Nd–O3^{a}	109.84(7)	O5–C6–C7	120.5(3)
O4–Nd–O3^{a}	50.81(6)	O6–C6–C7	119.8(3)
O3–Nd–O1^{b}	122.37(7)	C6–C7–C8	114.1(3)
O1–Nd–O1^{b}	66.75(8)	C7–C8–C7^{e}	111.9(4)

[a] Symmetry transformations used to generate equivalent atoms: [a] $-x, -y, -z+1$; [b] $-x+1, -y, -z+1$; [c] $x+1/2, y-1/2, z$; [d] $-x+1/2, -y-1/2, -z+1$; [e] $-x, y, -z+1/2$.

Centre (CCDC). See Information for Authors, *J. Mater. Chem.*, 1998, Issue 1. Any request to the CCDC for this material should quote the full literature citation and the reference number 1145/120.

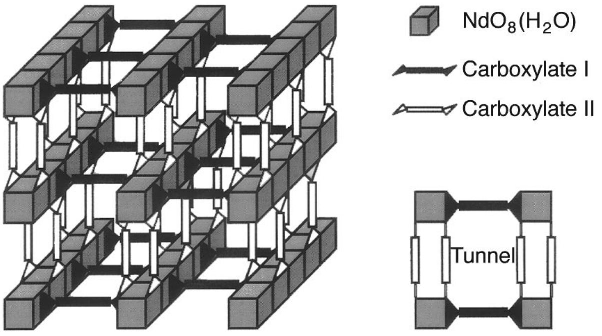

Fig. 2 Schematic of the open framework of $[Nd(H_2O)]_2[O_2C(CH_2)_3CO_2]_3 \cdot 4H_2O$ showing neodymium chains linked along two directions by two types of carboxylates, in order to form tunnels along the metal chains.

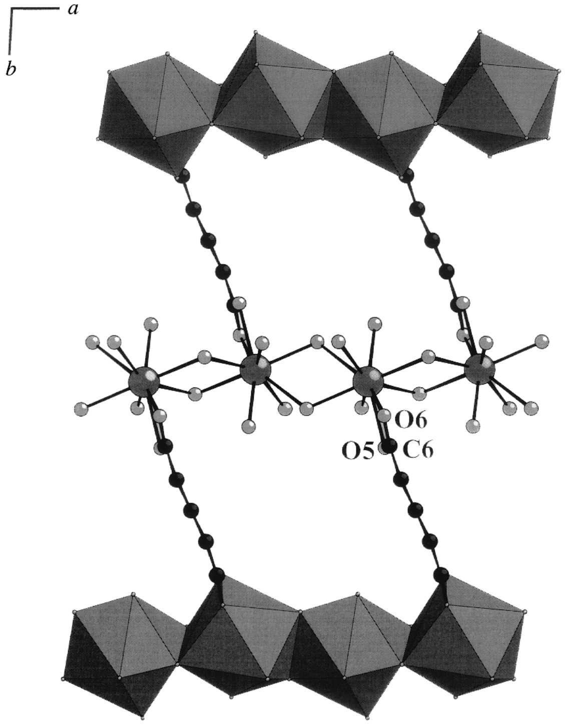

Fig. 3 Projection of the structure of $[Nd(H_2O)]_2[O_2C(CH_2)_3CO_2]_3 \cdot 4H_2O$ along the [011] direction showing the linkage of the chains of neodymium polyhedra by the carbon chains (in black) along the [101] direction (other carbon atoms, free water molecules and hydrogen atoms have been omitted for more clarity).

Results

Structure of $[Nd(H_2O)]_2[O_2C(CH_2)_3CO_2]_3 \cdot 4H_2O$

The structure of $[Nd(H_2O)]_2[O_2C(CH_2)_3CO_2]_3 \cdot 4H_2O$ is three-dimensional, consisting of chains of edge-sharing $NdO_8(H_2O)$ polyhedra, along the [100] direction, linked together by the carbon chains along the [010] and roughly [101] directions. The complex connection, schematized in Fig. 2, involves the formation of small channels along the [100] direction (with free aperture 3.3 Å and parallel to the neodymium polyhedra chains), in which weakly bonded water molecules are incorporated.

As highlighted in Fig. 2, there are two types of carboxylates, in the ratio 1:2. The first type (carboxylate I, black in the

Table 4 Cell parameters, unit cell volume, and calculated densities for $[M(H_2O)]_2[O_2C(CH_2)_3CO_2]_3 \cdot 4H_2O$ (M = Pr, Nd, Sm, Eu, Gd, Dy, Ho or Y)

M	a/Å	b/Å	c/Å	β/degrees	V/Å^3	D_c/g cm^{-3}
Pr	8.1319(1)	15.1855(2)	19.8758(2)	93.732(0)	2449.2(1)	2.12
Nd	8.1174(1)	15.1841(3)	19.8803(3)	93.762(1)	2445.1(1)	2.14
Sm	8.0160(2)	15.0592(1)	19.7063(4)	93.940(1)	2373.2(1)	2.24
Eu	8.0161(3)	15.0740(5)	19.7237(6)	93.978(1)	2377.6(1)	2.24
Gd	7.9767(1)	15.0043(2)	19.6852(1)	94.326(1)	2349.3(1)	2.30
Dy	7.9516(1)	14.9801(2)	19.7034(3)	94.668(1)	2339.2(1)	2.34
Ho	7.9355(1)	14.9338(1)	19.6973(1)	94.808(1)	2327.6(1)	2.36
Y	7.9355(3)	14.9438(6)	19.6973(8)	94.808(1)	2327.6(3)	1.93

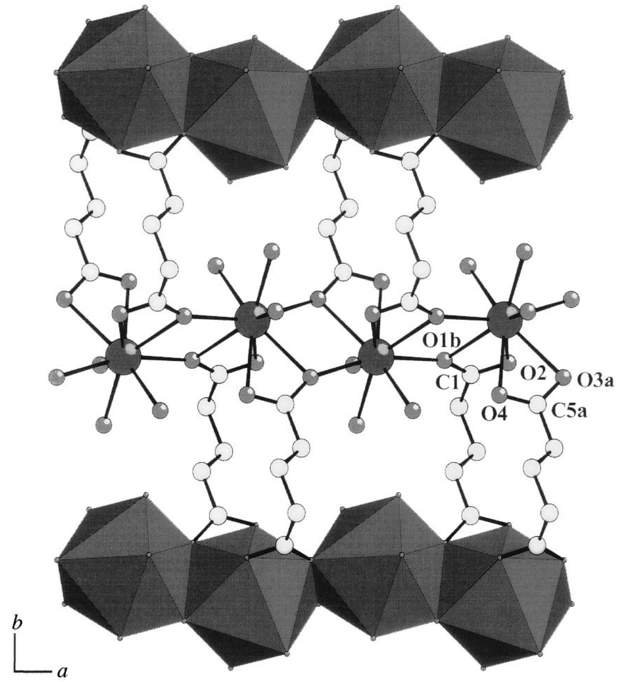

Fig. 4 Projection of the structure of $[Nd(H_2O)]_2[O_2C(CH_2)_3\text{-}CO_2]_3{\cdot}4H_2O$ along the [001] direction showing the linkage of the chains of neodymium polyhedra by the carbon chains (in white) along the [010] direction (other carbon atoms, free water molecules and hydrogen atoms have been omitted for more clarity).

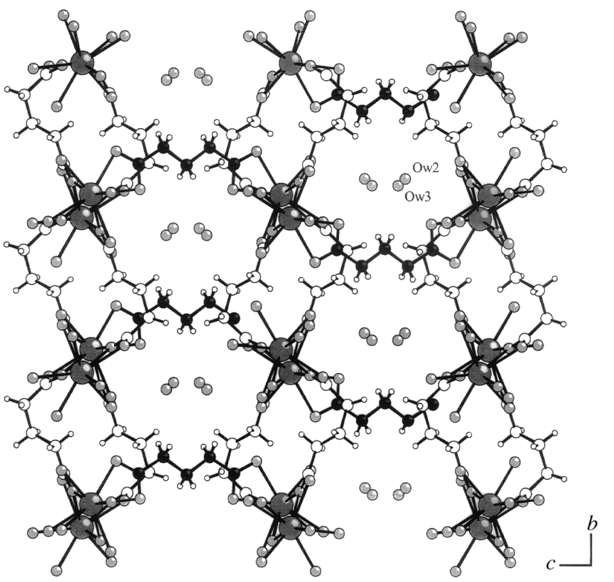

Fig. 5 Projection of the structure of $[Nd(H_2O)]_2[O_2C(CH_2)_3\text{-}CO_2]_3{\cdot}4H_2O$ along the [100] direction showing the channels and water molecules within them (for a better distinction between the carbon chains, both types of chains are represented in white and black, according to Fig. 3 and 4).

figures), which connect the chains along the [101] direction, simply chelates one neodymium atom at each end, as shown in Fig. 3. The second type (carboxylate II, white in the figures) which ensures the linkage of the chains along the [010] direction chelates a metal atom but one of the chelating oxygen atoms is also shared with an adjacent metal atom, as shown in Fig. 4. Examination of the C–O distances shows two types of $-CO_2^-$ carboxylate groups: both $-C1O1^bO2^-$ and $-C5^aO3^aO4^-$, which belong to carboxylate II, exhibit one short [C1–O2 1.257(3), C5^a–O4 1.264(3) Å] and one longer distance [C1–O1^b 1.288(3), C5^a–O3^a 1.282(3) Å], due to three-coordinated O1^b and O3^a oxygen atoms, bonded to two neodymium atoms and carbon; in the chelating $-C6O5O6^-$ carboxylic group (carboxylate I), the C6–O5 and C6–O6 distances are equivalent [1.270(3) and 1.278(3) Å, respectively]. The chelating and bridging effects of the carboxylic groups can also be evidenced by FTIR analysis. Indeed, the bands observed in the range 1600–1400 cm^{-1} (1536 cm^{-1}, 1445 and 1411 cm^{-1}) can be assigned to $\nu_{C=O}$ and ν_{C-O} vibrations for bridging and chelating carboxylic groups, as Deacon and Phillips showed for metal acetates and trifluoroacetates.[14] The whole arrangement leads to the formation of an open framework, as shown in Fig. 5 and 6. The channels are elliptical with free aperture $d_{min} \approx 3$ Å (between two H atoms, $R_H = 1.1$ Å) by $d_{max} \approx 5$ Å (between two O atoms, $R_O = 1.5$ Å). Such dimensions do not allow any porosity.

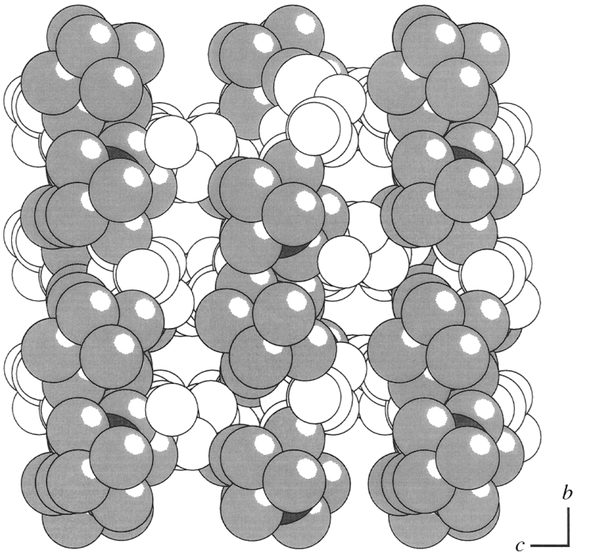

Fig. 6 Space filling representation of the structure of $[Nd(H_2O)]_2[O_2C(CH_2)_3CO_2]_3{\cdot}4H_2O$ showing the open framework with small channels along the [100] direction.

Two Nd–Nd distances, 4.20(1) and 4.28(1) Å occur in the chains. The neodymium atoms are nine-coordinated by one water molecule (Ow1) and eight oxygen atoms from five carboxylic groups, as shown in Fig. 7. Three carboxylate groups chelate the metal atom while two other carboxylate

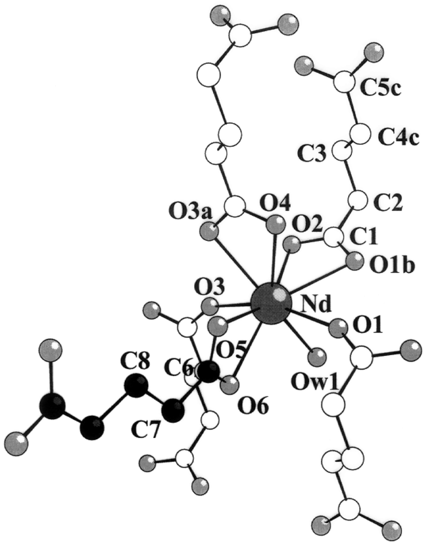

Fig. 7 Representation of the coordination about the neodymium atom in $[Nd(H_2O)]_2[O_2C(CH_2)_3CO_2]_3{\cdot}4H_2O$ including the numberings scheme used in the Tables.

groups share only one bridging oxygen atom. The angles formed at the neodymium atom by the chelate rings are quite small [O5–Nd–O6 52.1(1), O2–Nd–O1^b 50.3(1), O4–Nd–O3^a 50.8(1)°], leading to a highly distorted polyhedron around the neodymium. Moreover, each chelate ring has one short and one longer Nd–O bond [Nd–O2 2.50(1) and Nd–O1^b 2.67(1) Å, Nd–O4, 2.53(1) and Nd–O3^a 2.60(1) Å]. The presence of water molecules seen by the X-ray analysis and indicated by bond valence calculations[15] is confirmed by TG analysis, the curve indicating two successive weight losses of 7.4 and 4.6 wt.% in the ranges 30–100 and 100–200 °C, which can be attributed to the loss of free water molecules Ow2 and Ow3 (9.2 wt.%) and coordinating water molecule Ow1 (4.6 wt.%), respectively. The final residue at 900 °C is the neodymium oxide Nd_2O_3. The compound is able to reversibly adsorb and desorb free water molecules in the temperature range 25–100 °C; the study of this behaviour will be reported elsewhere.[16]

Acknowledgements

We are grateful to Dr. T. Loiseau for the X-ray data collection and Rhodia for financial support.

References

1 G. Férey, *J. Fluorine Chem.*, 1995, **72**, 187 and references therein; *C. R. Acad. Sci. Sér. C*, 1998, **2**, 1 and references therein.

2 M. Haouas, C. In-Gérardin, F. Taulelle, C. Estournes, T. Loiseau and G. Férey, *J. Phys. Chem.*, 1998, **95**, 320.

3 D. Riou and G. Férey, *J. Solid State Chem.*, 1994, **111**, 422; D. Riou, F. Taulelle and G. Férey, *Inorg. Chem.*, 1996, **35**, 6392; M. Cavellec, D. Riou, C. Ninclaus, J.-M. Grenèche and G. Férey, *Zeolites*, 1996, **17**, 250; M. Cavellec, D. Riou, J.-M. Grenèche and G. Férey, *J. Magn. Magn. Mater.*, 1996, **163**, 173; M. Cavellec, J.-M. Grenèche, D. Riou and G. Férey, *Microporous Mater.*, 1997, **8**, 103; M. Cavellec, J.-M. Grenèche and G. Férey, *Microporous Mater.*, 1998, **20**, 45; M. Cavellec, C. Egger, J. Linares, M. Nogues, F. Varret and G. Férey, *J. Solid State Chem.*, 1997, **134**, 349.

4 A. Clearfield, *Curr. Opin. Solid State Mater. Sci.*, 1996, **1**, 268 and references therein.

5 M. E. Thompson, *Chem. Mater.*, 1994, **6**, 1168 and references therein.

6 G. Alberti, U. Costantino, F. Marmottini, R. Vivani and P. Zappelli, *Angew. Chem.*, *Int. Ed. Engl.*, 1993, **32**, 1357; G. Alberti, F. Marmottini, S. Murcia-Mascarós and R. Vivani, *Angew. Chem.*, *Int. Ed. Engl.*, 1994, **33**, 1594; L. A. Vermeulen and M. E. Thompson, *Chem. Mater.*, 1994, **6**, 77; V. Soghomonian, Q. Chen, R. C. Haushalter and J. Zubieta, *Angew. Chem.*, *Int. Ed. Engl.*, 1995, **34**, 223; V. Soghomonian, R. Diaz, R. C. Haushalter, C. J. O'Connor and J. Zubieta, *Inorg. Chem.*, 1995, **34**, 4460; H. Byrd, A. Clearfield, D. Poojary, K. P. Reis and M. E. Thompson, *Chem. Mater.*, 1996, **8**, 2239; D. M. Poojary, B. Zhang, P. Bellinghausen and A. Clearfield, *Inorg. Chem.*, 1996, **35**, 4942; 5254; G. Bonavia, R. C. Haushalter, C. J. O'Connor and J. Zubieta, *Inorg. Chem.*, 1996, **35**, 5603; P. J. Zapf, D. J. Rose, R. C. Haushalter and J. Zubieta, *J. Solid State Chem.*, 1996, **125**, 182; D. L. Lohse and S. C. Sevov, *Angew. Chem.*, *Int. Ed. Engl.*, 1997, **36**, 1619.

7 S. Drumel, P. Janvier, P. Barboux, M. Bujoli-Doeuff and B. Bujoli, *Inorg. Chem.*, 1995, **34**, 148; S. Drumel, P. Janvier, D. Deniaud and B. Bujoli, *J. Chem. Soc.*, *Chem. Commun.*, 1995, 1051.

8 J. W. Bats, R. Kalus and H. Fuess, *Acta Crystallogr.*, *Sect. B*, 1979, **35**, 1225; M. C. Favas, D. L. Kepert, B. W. Skelton and A. H. White, *J. Chem. Soc.*, *Dalton Trans.*, 1980, **54**; M. S. Khiyalov, I. R. Amiraslanov, F. N. Musaev and Kh. S. Mamedov, *Koord. Khim.*, 1982, **8**, 548; H. Gries and H. Miklautz, *Physiol. Chem. Phys. Med. NMR*, 1984, **16**, 105; M. S. Konings, W. C. Dow, D. B. Love, K. N. Raymond, S. C. Quay and S. M. Rocklage, *Inorg. Chem.*, 1990, **29**, 1448; M. A. J. Moss and C. J. Jones, *J. Chem. Soc.*, *Dalton Trans.*, 1990, 581; D. Zhi-Bang, J. Zhing-Sheng, W. Ge-Cheng and N. Jia-Zan, *J. Struct. Chem.*, 1990, **9**, 64; L. Ehnebom and B. F. Pedersen, *Acta Chem. Scand.*, 1992, **46**, 126; S. J. Franklin and K. N. Raymond, *Inorg. Chem.*, 1994, **33**, 5794; C. Daiguebonne, Y. Gerault, O. Guillou, A. Lecerf, K. Boubekeur, P. Batail, M. Khan and O. Khan, *International Conference on f Elements 3*, Paris, France, 1997.

9 S. Romero, A. Mosset and J. C. Trombe, *Eur. J. Solid State Inorg. Chem.*, 1997, **34**, 209 and references therein.

10 *Handbook of Chemistry and Physics*, Boca Raton, FL, 77th edn., 1996.

11 G. M. Sheldrick, SADABS, a program for the Siemens Area Detector ABSorption correction, 1994.

12 R. Blessing, *Acta Crystallogr.*, *Sect. A*, 1995, **51**, 33.

13 G. M. Sheldrick, SHELXTL version 5.03, software package for the Crystal Structure Determination, 1994.

14 G. B. Deacon and R. J. Phillips, *Coord. Chem. Rev.*, 1980, **33**, 227.

15 N. E. Brese and M. O'Keeffe, *Acta Crystallogr.*, *Sect. B*, 1991, **47**, 192.

16 F. Serpaggi, T. Luxbacher, A. K. Cheetham and G. Férey, *J. Solid State Chem.*, submitted.

Paper 8/02713G